Yeast genome-wide drug-induced haploinsufficiency screen to determine drug mode of action

Kristin Baetz*, Lianne McHardy†, Ken Gable‡, Tamsin Tarling†, Delphine Rebérioux†, Jenny Bryan§¶, Raymond J. Andersen‖, Teresa Dunn‡, Phil Hieter*†¶, and Michel Roberge†**

*Centre for Molecular Medicine and Therapeutics, Vancouver, BC, Canada V5Z 4H4; ¶Biotechnology Laboratory and Departments of †Biochemistry and Molecular Biology, §Statistics, and ‖Earth-Ocean Sciences and Chemistry, University of British Columbia, Vancouver, BC, Canada V6T 1Z3; and ‡Department of Biochemistry, Uniformed Services University of the Health Sciences, Bethesda, MD 20814

Edited by Francis S. Collins, National Institutes of Health, Bethesda, MD, and approved January 21, 2004 (received for review November 3, 2003)

Methods to systematically test drugs against all possible proteins in a cell are needed to identify the targets underlying their therapeutic action and unwanted effects. Here, we show that a genome-wide drug-induced haploinsufficiency screen by using yeast can reveal drug mode of action in yeast and can be used to predict drug mode of action in human cells. We demonstrate that dihydromotuporamine C, a compound in preclinical development that inhibits angiogenesis and metastasis by an unknown mechanism, targets sphingolipid metabolism. The systematic, unbiased and genome-wide nature of this technique makes it attractive as a general approach to identify cellular pathways affected by drugs.

Cell-based screening is increasingly used to identify chemicals that can suppress or enhance particular cellular phenotypes. Chemicals identified by phenotypic screening are valuable chemical genetic tools to study complex cellular processes and are often attractive candidates for drug development (1–3). Identification of the mechanism of action of these chemicals is an integral part of the chemical genetic approach and is also critical for evaluating and optimizing therapeutic agents, yet no systematic target identification approach exists (3). The classical method is to purify the target from cellular extracts by using immobilized or radiolabeled versions of the chemical or to guess candidates and test them one by one in binding or functional assays (3). However, without prior knowledge of the pathways affected by the drug, these approaches have met with little success and systematic genomic and proteomic methods to test a wide range of drugs against all possible targets in a cell are clearly needed.

The budding yeast *Saccharomyces cerevisiae* has been proposed as a tool for identifying human drug targets because >40% of yeast proteins share some conserved sequence with at least one known or predicted human protein, including several hundred genes implicated in human disease (4, 5). Recent technological advances in yeast genomics, including gene expression profiling, chemical-genetic synthetic profiling, and drug-induced haploinsufficiency, show promise as tools to study proteins and pathways affected by drugs at a genome-wide level (4, 5). Drug-induced haploinsufficiency occurs when lowering the dosage of a single gene from two copies to one copy in diploid cells results in a heterozygote that displays increased drug sensitivity compared with wild-type strains (6). Giaever *et al.* (6) pooled 233 "bar-coded" heterozygous yeast strains, grew them competitively in the presence of a drug whose target in yeast cells was known, and successfully used DNA microarrays to identify the heterozygous drug target strain whose growth was compromised in the presence of the drug. Here, we asked whether drug-induced haploinsufficiency could be applied genome-wide to identify the mode of action of a drug with an unknown target. We used dihydromotuporamine C (dhMotC) (Fig. 1*A*), a member of the motuporamine family of agents discovered in a phenotypic screen for small molecules that inhibit invasion of human carcinoma cell lines (2, 7). The motuporamines inhibit the formation of invadopodia, decrease tumor cell motility, and alter the organization of filamentous actin at the cell margin (2). Identifying the mechanism of action of dhMotC is critical for evaluating its potential for cancer therapy but it is a difficult task, because dhMotC has no other known biological activities, it does not resemble other bioactive molecules, and its chemical structure revealed no clues to guide target identification.

By using a genome-wide haploinsufficiency screen, we show that dhMotC targets sphingolipid metabolism, resulting in decreased ceramide levels in yeast. Furthermore, exogenous ceramide partially rescues the effect of dhMotC on human cell survival, demonstrating that systematic genome-wide analysis of drug effects in yeast can be used to elucidate the mechanism of action of drugs in yeast and in human cells.

Materials and Methods

Reagents. dhMotC was a generous gift of D. Williams (University of British Columbia). It was synthesized as described (7) and was solubilized in DMSO. Dihydrosphingosine (DHS) and C6-ceramide were purchased from Sigma.

Yeast Strains, Media, and Genetic Manipulations. The diploid heterozygous deletion mutants generated by the International Deletion Consortium (8) were obtained from Research Genetics/Invitrogen. BY4743 was used as the diploid wild-type control. TDY2037 (wild-type) and TDY2038 (*csg2*Δ) *MAT*α haploid strains were described (9). Yeast was grown on standard rich medium [yeast extract/peptone/dextrose (YPD)] as described (10).

Individual Growth Rate Analysis. Growth rates of strains were measured under various drug conditions essentially as described (6). Cells were diluted from an overnight culture to an OD_{600} of ≈0.01 and were allowed to grow until the OD_{600} reached ≈0.05 ($t = 0$) to ensure that cells were in logarithmic phase. Drug was added and growth rates were measured by determination of OD_{600} as a function of time by using a Pharmacia Biotech Ultrospec 3000 or a Tecan Sunrise plate reader. Growth curves were carried out in triplicate and curves shown are averages of three experiments with error bars representing 1 SD.

Drug-Induced Haploinsufficiency Screen. The deletion mutant arrays (DMA) were propagated on rich liquid medium containing G418 (200 mg/liter, GIBCO/BRL). The DMA were transferred by hand with a model VP408FH 96-floating pin replicator (V & P Scientific, San Diego) and a VP380 colony copier (V & P Scientific) into 96-well plates containing 100 μl of liquid YPD and were grown overnight at 25°C to saturation. Replicator

GENETICS

This paper was submitted directly (Track II) to the PNAS office.

Abbreviations: dhMotC, dihydromotuporamine C; DHS, dihydrosphingosine; IGCD, integrative growth curve difference; YPD, yeast extract/peptone/dextrose; LCB, long chain base; Tsc10, 3-ketosphinganine reductase.

**To whom correspondence should be addressed. E-mail: michelr@interchange.ubc.ca.

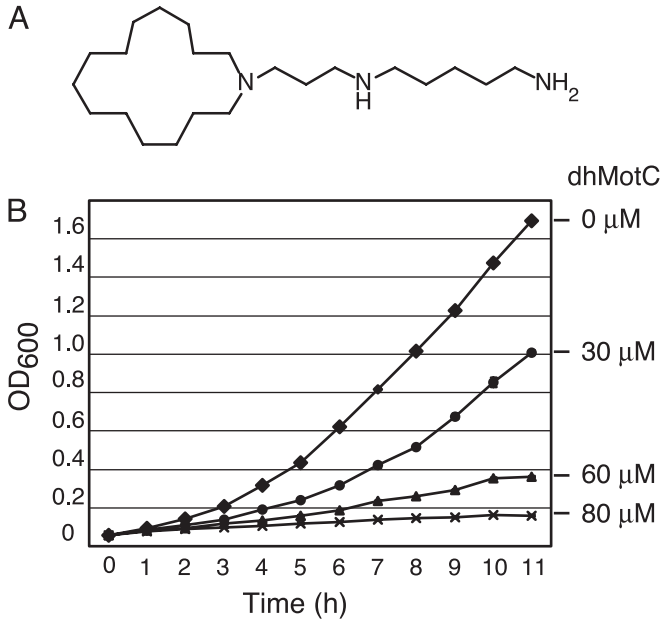

Fig. 1. Sensitivity of yeast to dhMotC. (*A*) Structural formula of dhMotC. (*B*) Growth of wild-type (BY4743) strain (OD_{600}) as a function of time in hours. BY4743 was grown in YPD liquid culture with or without dhMotC treatment as indicated. Growth curves were performed in triplicate and represent the average of three experiments.

sterilization procedures were as described (11). Saturated cultures compensated for differences in growth rate between strains, to ensure that roughly equal amounts of cells were deposited on the agar plates. After 24 h, the DMA were pinned onto plates (OmniTray, Nunc) containing YPD-agar and DMSO (6 μl/ml) or 60 μM dhMotC and DMSO (6 μl/ml). DMA were arrayed at high density by using a BioRobotics TAS1 robot with a 0.4-mm diameter 96-pin tool that spots ≈20 nl or ≈250 cells. Strains were pinned in duplicate with a density of 1,536 per plate. Pins were sterilized by agitating for 30 s in 10% bleach followed by 95% ethanol for 15 s and drying with warm air for 15 s. Plates were grown at 25°C and strains were scored for growth, slow growth, or no growth, compared with no drug over a period of 4 days.

Integrative Growth Curve Difference (IGCD) Analysis. We analyzed growth curves for 29 strains, each grown without drug and in the presence of 20 μM dhMotC. OD_{600} measurements of cell density were taken hourly for 10 time points. The typical level of replication was three growth curves per strain per condition, for a total of six curves per strain. The cultures underwent exponential growth during the time points and conditions studied. Therefore, we used a log-transformed linear model to relate growth to time by using the model: $\log OD_{600\,g}(t) = \beta_{0g} + \beta_{1g} M + \beta_{2g} t + \beta_{3g} tM + \varepsilon_g$ where g indicates the strain, M indicates the presence of dhMotC, and t indicates time. The intercept of this model, equal to $\beta_{0g} + \beta_{1g} M$, captures early growth and β_{1g} is the adjustment due to dhMotC. The slope, equal to $\beta_{2g} + \beta_{3g} M$, reflects the steady-state doubling time and β_{3g} is the adjustment due to dhMotC. Both the intercept and the slope were modified by the presence of dhMotC, indicating early and persistent effects on growth, respectively. The dhMotC effect on growth was highly statistically significant ($P < 10^{-11}$) for all 29 strains evaluated, when quantified by using an F test for a restricted model that does not include the dhMotC terms. Strains were ranked according to the cumulative dhMotC effect or IGCDs, denoted D_g, as measured by the area between the expected growth curves with and without drug. Because these curves were linear on the transformed scale, the integral has the following simple form $D_g = (-T\beta_{1,g} - T^2/2)\,\beta_{3,g}$. Therefore, the final quantitative measure of cumulative dhMotC effect on each strain is the estimated value of D_g, obtained by evaluating the above expression at the estimated dhMotC regression coefficients.

Immunolocalization Studies. Cells were grown to early log phase in YPD at 25°C and treated with either DMSO, 60 μM dhMotC, or 60 μM dhMotC plus 50 μM DHS for 1.5 h. Cells were then fixed in formaldehyde and were stained with rhodamine-phalloidin (R-415, Molecular Probes) to visualize F-actin and 4′,6-diamidino-2-phenylindole (Sigma) to visualize DNA as described (12).

Whole-Cell Ceramide Isolation. Wild-type (TDY2037) and *csg2*Δ (TDY2038) cells were grown overnight in YPD to an OD_{600} near 1.0. Cells were diluted to 0.2–0.4 OD_{600} in YPD containing 10 μCi/ml (1 Ci = 37 GBq) ^{3}H-serine and were treated with either 5 μM dhMotC or the equivalent amount of DMSO. After 8 h, 12 OD_{600} units of cells were harvested by centrifugation, were washed with water, were dried thoroughly, and 20 volumes of hexane:ethanol (95:5) were added. The cells were extracted by bead beating and bath sonication. The resulting suspension was centrifuged to remove cell debris. The hexane:ethanol fraction was dried under nitrogen and was subjected to mild alkaline hydrolysis in ethanol:water:ether:pyridine (15:15:5:1) with 0.1 M KOH added. After 3 h at 37°C, the solution was neutralized by the addition of 0.1 M acetic acid and was dried under nitrogen. The dried extract was desalted by resuspension in water-saturated butanol. An equal volume of water was added and the butanol layer was extracted after centrifugation and was dried under nitrogen. A total of 10 OD_{600} of each sample were run on TLC plates by using chloroform:methanol:acetic acid (95:4.5:0.5), the TLC plates were dried, and were rerun on the same system. After the second run, the plates were sprayed with 10% $CuSO_4$ in 8% phosphoric acid, were dried completely, and were heated at 80° until the ceramide was visible. The ceramide bands were scraped off the TLC plate and the amount of serine incorporated into ceramide was determined by liquid scintillation counting.

Mammalian Cell Survival Assay. MDA-231 cells were plated at 10,000 cells per well in 96-well culture dishes and were allowed to grow overnight. They were subsequently exposed to different concentrations of dhMotC and/or C6-ceramide (Sigma) for 24 h. Cell survival was measured by using the (3-(4,5-dimethylthiazolyl-2)-2,5-diphenyltetrazolium bromide) assay (Sigma).

Database. For further information, refer to the *Saccharomyces* Genome Database, which can be accessed at www.yeastgenome.org.

Results

We developed a pathway/target identification procedure by using drug-induced haploinsufficiency in yeast that consists of five stages: (*i*) selection of a drug-induced phenotype; (*ii*) systematic high-throughput phenotypic screen of a yeast heterozygous deletion diploid set for enhanced or suppressed drug-induced phenotype; (*iii*) selection of potential pathways/targets based on quantitative ranking of drug sensitivity; (*iv*) confirmation of drug mode of action in yeast; and (*v*) assessment of cognate mode of action in the mammalian system.

Sensitivity of Yeast to dhMotC. As a prerequisite, treatment of yeast with a drug of interest must cause a phenotype that is easily scored, such as growth inhibition. dhMotC inhibited the growth

Table 1. Heterozygous deletion strains sensitive to dhMotC

ORF	Name	Biological process†
YCL034W	*LSB5*	Actin filament organization
YNL314W	*DAL82*	Allantoin catabolism and transcription initiation from polymerase II promoter
YML099C	*ARG81*	Arginine metabolism
YBR078W	*ECM33*	Cell wall organization and biogenesis
*YNL267W**	*PIK1**	Cytokinesis, post-Golgi transport, and signal transduction
YLR286C	*CTS1*	Cytokinesis, completion of separation
YDL192W	*ARF1*	ER-to-Golgi transport and intra-Golgi transport
YBR290W	*BSD2*	Heavy metal ion transport and protein vacuolar targeting
YLR025W	*SNF7*	Late endosome to vacuole transport
YHR147C	*MRPL6*	Protein biosynthesis
*YOL040C**	*RPS15**	Protein biosynthesis
YAL005C	*SSA1*	Protein folding and protein-nucleus import, translocation
YIL047C	*SYG1*	Signal transduction
*YBR265W**	*TSC10**	Sphingolipid biosynthesis
*YMR296C**	*LCB1**	Sphingolipid biosynthesis
*YJR007W**	*SUI2**	Translation initiation
*YML092C**	*PRE8**	Ubiquitin-dependent protein catabolism
YER140W	*YER140W*	Unknown
YER188W	*YER188W*	Unknown
YGR205W	*YGR205W*	Unknown
YLR294C	*YLR294C*	Unknown

*Essential genes.
†Biological process according to their *Saccharomyces* Genome Database report.

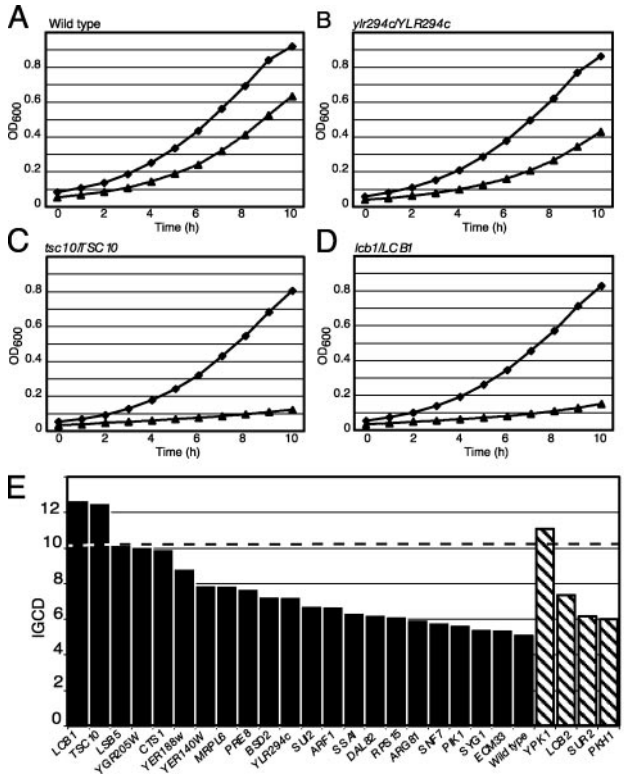

Fig. 2. dhMotC sensitivity of heterozygous deletion strains identified in the high-throughput screen. (*A–D*) Growth of wild-type (*A*), *ylr294/YLR294* (*B*), *tsc10/TSC10* (*C*), and *lcb1/LCB1* (*D*) strains as a function of time in hours in YPD liquid culture under two conditions: ♦, no drug control (DMSO); ▲ 20 μM dhMotC. Growth curves were preformed in triplicate, and OD_{600} was measured by using a Tecan Sunrise plate reader. Growth curves represents the average of three experiments. (*E*) Plot of the IGCD for 21 heterozygous deletion strains identified in the drug screen are represented by black bars. The IGCD levels for the three additional heterozygous strains in the sphingolipid pathway sensitive to dhMotC are represented by gray bars. The dashed line represents 2-fold IGCD level used to define supersensitive strains.

of wild-type diploid yeast (BY4743) in liquid cultures in a concentration-dependent manner (Fig. 1*B*). Concentrations >60 μM severely inhibited growth and resulted in a terminal phenotype that was not cell cycle-specific (data not shown). This result suggests that dhMotC targets at least one gene product involved in an essential function in *S. cerevisiae*.

Genome-Wide Drug-Induced Haploinsufficiency Screen. For high-throughput phenotypic screening, a set of >5,000 heterozygous diploid deletion strains covering most yeast genes was robotically arrayed onto agar plates containing either DMSO (no drug control) or a sublethal dhMotC concentration of 60 μM. The plates were incubated at 25°C and strain growth on DMSO- and dhMotC-treated plates was compared over a period of 4 days. An extended monitoring period was necessary for scoring of strains that grew slowly because of their intrinsic haploinsufficiency. The screen was carried out twice and strains displaying increased sensitivity to dhMotC in both screens are shown in Table 1. The list includes six essential genes and 15 nonessential genes implicated in a variety of functions.

Quantitative Identification of Supersensitive Strains. To confirm and quantitatively rank the sensitivity of the 21 strains, we carried out automated quantitative liquid growth measurements under no-drug conditions or at a concentration of dhMotC (20 μM) that causes only a small degree of growth inhibition (Fig. 2*A*). Because many heterozygous yeast deletion strains exhibit a slow growth phenotype or haploinsufficiency in rich culture medium (6), it was necessary to compare growth profiles with and without drug for each strain. We next established a model for ranking strain sensitivity by using IGCDs (see *Materials and Methods*), a technique unbiased by differences in growth rate between strains.

As expected, all 21 strains were more sensitive to 20 μM dhMotC than the wild-type control, but most showed only minor growth inhibition. However, two strains were clearly more sensitive than others: *lcb1*Δ/LCB1 and *tsc10*Δ/TSC10 showed an IGCD >2-fold over wild type and were defined as supersensitive (Fig. 2 *C* and *D*). Eight additional strains showed IGCD >1.5-fold greater than wild type (Fig. 2*E*). Both *LCB1* and *TSC10* are essential genes required for the biosynthesis of the sphingolipid precursor sphingosine, suggesting that dhMotC targets a sphingolipid-dependent process.

dhMotC Targets Sphingolipid Biosynthesis. Sphingolipids are essential components of all eukaryotic cells, playing both structural and regulatory roles (13, 14). The first committed step of sphingolipid synthesis is the condensation of serine and palmitoyl CoA to 3-ketodihydrosphingosine catalyzed by serine palmitoyl transferase, composed of subunits encoded by *LCB1* and *LCB2*. The quantity of 3-ketodihydrosphingosine is then reduced to DHS by 3-ketosphinganine reductase (Tsc10) encoded by *TSC10* and DHS is subsequently hydroxylated to phytosphingosine (PHS) by DHS hydroxylase encoded by *SUR2.* PHS is conjugated with C26-fattyacyl-CoA to form ceramide in a reaction requiring the homologous and functionally redundant *LAG1* and *LAC1* (Fig. 3). In mammalian cells, the predominant long

GENETICS

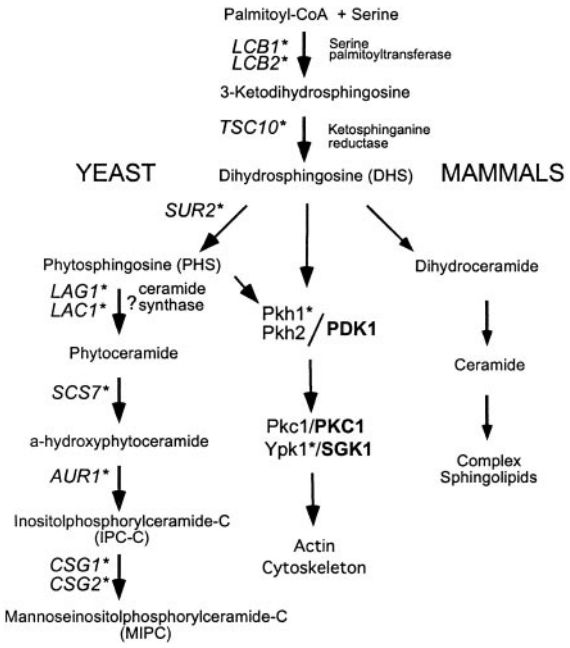

Fig. 3. Schematic diagram of sphingolipid biosynthesis and sphingosine-dependent kinase cascade in yeast and humans. Yeast genes are italic, and yeast proteins are Roman. Human proteins are bold. Heterozygous yeast strains tested for sensitivity to dhMotC are indicated by asterisks.

chain base (LCB) is sphingosine (formed by desaturation of DHS) rather than PHS. In addition to *de novo* synthesis, LCBs and ceramide are produced both by this synthetic pathway and by catabolism of complex sphingolipids that are major components of cellular membranes. Sphingosine also plays an intracellular signaling function by activating a Pkh1-Ypk1 kinase cascade controlling the actin cytoskeleton (Fig. 3 and refs. 13 and 14). Pkh1 phosphorylates and activates several protein kinases, including Ypk1 and Pkc1 (15, 16). *PKH1* is a nonessential gene that is genetically redundant with *PKH2*, and *pkh1*Δpkh2Δ double-deletion mutants are inviable (15, 16), whereas $pkh1^{D398G}pkh2\Delta$ double mutants are viable and display actin polarization defects (16). Although no genes of the sphingolipid metabolism pathway other than *LCB1* and *TSC10* were identified in the high-throughput screen, the supersensitivity of *lcb1*Δ/LCB1 and *tsc10*Δ/TSC10 to dhMotC motivated us to directly test the sensitivity of additional heterozygous mutants (indicated in Fig. 3). Whereas most strains did not display dhMotC sensitivity above wild type, the *ypk1*Δ/*YPK1* strain was supersensitive and lcb2Δ/*LCB2*, *sur2*Δ/SUR2, and *pkh1*Δ/PKH1 strains showed increased sensitivity to dhMotC when tested in the liquid growth assay (Fig. 2*E*). The sensitivity of six mutants heterozygous for deletions of genes involved in sphingolipid metabolism strongly suggests that dhMotC either directly targets sphingolipid metabolism or targets a pathway that is synthetically lethal in combination with compromised sphingolipid synthesis.

To determine whether interference with sphingolipid biosynthesis was important for growth inhibition by dhMotC, we asked whether increased levels of sphingolipid biosynthetic intermediates could rescue the dhMotC sensitivity of wild-type cells. Exogenous addition of DHS has been shown previously to rescue genetic disruption of *LCB1* (9, 17). We therefore tested the effect of DHS addition to liquid growth medium and found that DHS did not affect the growth of wild-type yeast but nearly completely suppressed growth inhibition by dhMotC (Fig. 4*A*). It has also been shown that lack of sphingosine synthesis results in defects in the organization of the actin cytoskeleton that can be rescued by exogenous DHS (17). Similarly, we found that dhMotC treatment caused depolarization of the yeast actin cytoskeleton, a defect that was also rescued by exogenous DHS (Fig. 4*B*). Deletion of either *CSG1* or *CSG2*, genes required for mannosylation of inositolphosphorylceramide-C, has been shown to cause the accumulation of inositolphosphorylceramide-C and ceramide in cells (18, 19). We found that *csg2*Δ mutant cells are almost completely resistant to dhMotC treatment, indicating that similar to exogenous DHS, elevated inositolphosphorylceramide-C and/or ceramide are protective against the effects of dhMotC (Fig. 4*C*).

Our analysis suggests that dhMotC directly affects the biosynthesis of sphingolipids in yeast. Therefore, we carried out biochemical assays to determine which sphingolipid metabolic intermediate might be affected by dhMotC. To address whether dhMotC directly inhibits Tsc10, we analyzed sphingoid bases from drug-treated cells. Whereas *tsc10* mutants (with reduced-function Tsc10) accumulate 3-ketosphinganine (9), treatment of cells with dhMotC did not cause 3-ketosphinganine to accumulate, nor did it alter the steady state levels of DHS and PHS (data not shown). Furthermore, *in vitro* activity of serine palmitoyl transferase was not inhibited by dhMotC (data not shown). These data indicate that dhMotC is not directly inhibiting serine palmitoyl transferase or Tsc10. However, dhMotC reduced cellular ceramide levels (data not shown). To investigate this hypothesis further, we measured incorporation of ^{3}H-serine into ceramide during an 8-h labeling period with and without dhMotC (Fig. 4*D*). Wild-type cells treated with sublethal levels of dhMotC have roughly half as much ceramide per cell after 8 h as untreated wild-type cells. As expected, *csg2*Δ cells have elevated levels of ceramide, and although dhMotC treatment of *csg2*Δ cells also lowers ceramide levels, ceramide levels are still above normal, confirming that elevated ceramide levels protect *csg2*Δ cells from dhMotC. The fact that dhMotC lowers ceramide levels in wild-type cells indicates that dhMotC directly targets sphingolipid metabolism in yeast rather than a pathway that is synthetic lethal with compromised sphingolipid metabolism.

If the mode of action of dhMotC is conserved between yeast and mammalian cells, then treatment of human cells with exogenous ceramide should rescue the effects of dhMotC. Exposure of breast carcinoma MDA-231 cells to high concentrations (10 μM) of dhMotC for an extended time (24 h) reduces their survival (Fig. 4*E*). Addition of 10 or 50 nM C6-ceramide had no effect on the survival of cells not exposed to dhMotC, but 10 nM C6-ceramide slightly increased survival and 50 nM C6-ceramide increased by 4- to 5-fold the survival of cells exposed to dhMotC (Fig. 4*E*). Higher ceramide concentrations reduced the extent of the rescue (data not shown), possibly because ceramide is known to induce apoptosis at higher concentrations (13, 20). These results indicate that modulation of ceramide levels by dhMotC is relevant to its mechanism of action in yeast and mammalian cells alike.

Discussion

We have applied a systematic approach for identifying candidate drug targets and pathways in yeast that should be applicable to any drug causing a scorable phenotype such as growth inhibition. Importantly, this study indicates that the physiological process that is affected by a drug in mammalian cells, in this case cancer cell invasion, need not be recapitulated in yeast for the technique to be considered. Of relevance is the cross-species conservation of biochemical pathway function and not the specific phenotypic consequence of pathway disruption in yeast versus human cells.

In this study, dhMotC was used as a test drug and the initial high-throughput screen identified 21 heterozygous deletion strains with increased sensitivity to dhMotC. Heterozygous gene deletions that cause increased drug sensitivity are expected to comprise essential genes whose products are direct drug targets and essential or nonessential genes that exhibit synthetic inter-

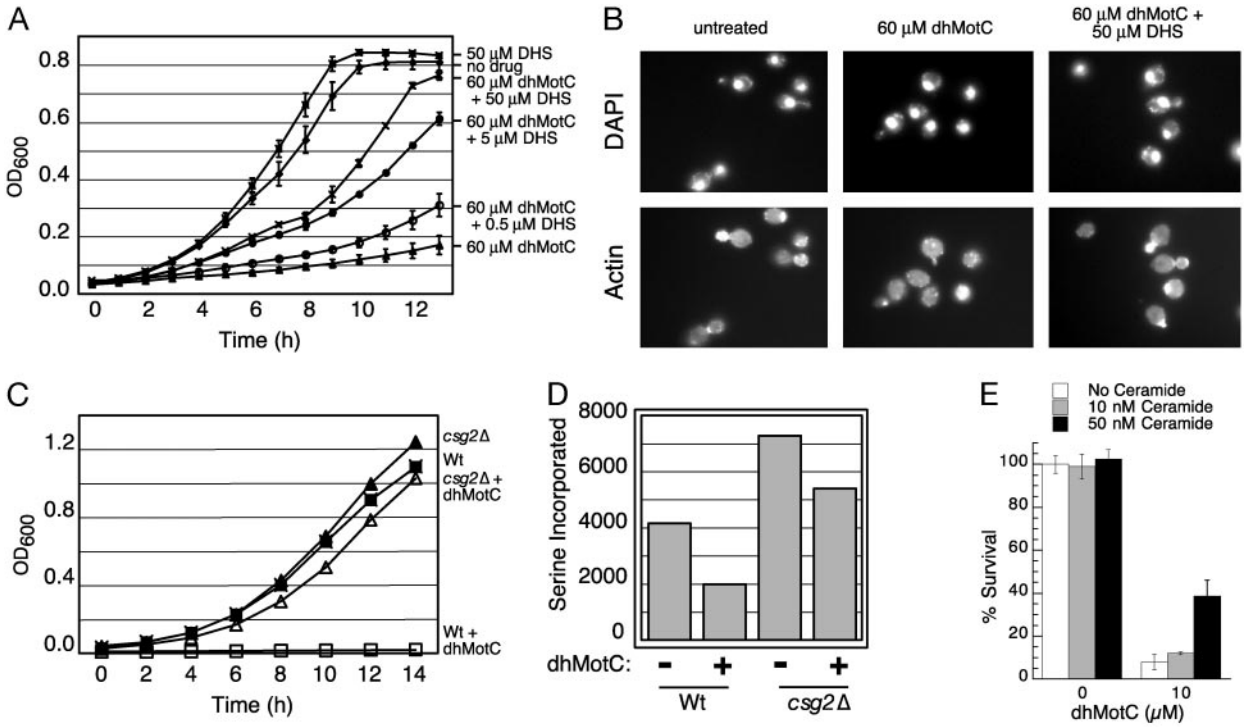

Fig. 4. dhMotC targets the sphingolipid biosynthesis pathway. (*A*) Growth of wild-type strain (BY4743, OD_{600}) as a function of time in YPD liquid culture with and without treatment of 60 μM dhMotC and increasing amounts of DHS as indicated. Growth curves were performed in triplicate and represent the average of three experiments. Treatment of yeast with DHS does not adversely affect the growth rate of yeast. (*B*) Actin staining in wild-type cells in the presence or absence of dhMotC. BY4743 cells were incubated at 25°C in the presence or absence of 60 μM dhMotC and 50 μM DHS as indicated for 1.5 h. The cells were then fixed, nuclear staining was visualized by using 4′,6-diamidino-2-phenylindole (*Upper*), and filamentous actin was visualized using rhodamine-phalloidin (*Lower*). (*C*) Growth of wild-type (TDY2037) and *csg2*Δ (TDY2038) haploid cells as a function of time in YPD liquid culture with and without 10 μM dhMotC treatment. Growth curves were performed in triplicate and represent the average of three experiments. Haploid cells have an increased sensitivity to dhMotC. (*D*) Incorporation of ^{3}H-serine into ceramide after 8 h was measured in both wild-type (TDY 2037) and *csg2*Δ (TDY 2038) cells with and without 5 μM dhMotC. (*E*) Rescue of dhMotC toxicity by ceramide in human cells. MDA-231 cell survival after 24-h exposure to 0 or 10 μM dhMotc and 0, 10, or 50 nM C6-ceramide is expressed as a percentage of untreated controls. The assay was performed in quadruplicate, and error bars represent 1 SD.

actions with the drug target. Quantitative ranking of dhMotC sensitivity in a subsequent liquid growth assay identified two members of the sphingolipid biosynthesis pathway, *lcb1*Δ/LCB1 and *tsc10*Δ/TSC10, as supersensitive strains, clearly prioritizing this pathway as the candidate target. Direct measurements of cellular sphingolipid levels showed that dhMotC treatment lowers ceramide levels. Artificially elevating ceramide levels by adding exogenous sphingosine or preventing the incorporation of ceramide into complex sphingolipids through *CSG2* inactivation nearly totally rescued the effects of dhMotC on yeast growth and on the actin cytoskeleton. These results demonstrate that inhibition of sphingolipid metabolism is the major, if not the sole mechanism, of action of dhMotC in yeast.

Our screen did not identify all genes of the sphingolipid metabolism pathway. Further iterations of the primary screen might have revealed additional ones, such as the supersensitive *ypk1*Δ/*YPK1* strain found in followup studies. However, functionally redundant genes such as *LAC1* and *LAG1* cannot be detected in simple haploinsufficiency screens, and other genes might escape detection because reduction in gene copy number does not manifest itself in compromised function. Despite these limitations, it is likely that at least a subset of heterozygous deletion strains of any given pathway will be gene dosage-sensitive and show supersensitivity to drugs in this assay, and will be sufficient to expose the pathway. The identification of highly sensitive heterozygous strains, such as *lsb5*Δ/LSB5 and *ygr205w*Δ/YGR205w, not known to be involved in sphingolipid biosynthesis might indicate that dhMotC has secondary targets, although the nearly complete rescue of dhMotC effects by exogenous sphingosine indicates they must be minor. It is also possible that lowered expression of these genes is synthetic lethal with compromised sphingolipid biosynthesis. This issue should be resolvable in the future, when complete synthetic genetic interaction maps are available to facilitate the sorting of genes into those that likely encode pathways targeted by drugs from those that display synthetic interactions with those pathways (21).

To determine whether yeast drug-induced haploinsufficiency screening is relevant for finding drug mode of action in human cells, we sought a simple test with broad applicability. Most drugs are expected to affect the survival of human cells at high doses. By analogy to the yeast growth inhibition experiments, we determined whether the deleterious effects of dhMotC on human cell survival could be rescued by addition of exogenous ceramide. Indeed, ceramide provided significant protection from the effects of dhMotC. However, the extent of protection was not as high as observed in yeast. One explanation is that dhMotC might have additional targets in human cells that are not present in yeast. Alternatively, because ceramide has been implicated in the regulation of numerous cellular pathways including apoptosis, senescence and cell-cycle arrest (13, 20), it is possible that rescue by exogenous ceramide is limited by its intrinsic toxicity. Nevertheless, this result provides crucial evidence that drug-induced haploinsufficiency studies in yeast can reveal pathways targeted by drugs in human cells.

In parallel to our own work, Lum *et al.* (22) have also presented a yeast drug-induced haploinsufficiency screen to identify drug mode of action by using a DNA microarray based method with similar results. The cell-based robotic screening procedure we

have presented can be adapted to screen numerous drug-induced phenotypes other than growth inhibition, such as activation of signaling pathways and of transcription, that are not easily amenable to DNA microarray-based screening. The systematic, unbiased and genome-wide nature of this technique makes it an attractive general tool both for discovering drug targets or mode of action and for revealing "targetable" biological pathways. Finding new starting points for intervention will contribute to the development of new therapeutic approaches to disease, a major stated goal of the Human Genome Project (23).

We thank David Williams for providing dhMotC; Vivien Measday and Hilary Anderson for critically reading the manuscript and for advice; Crystal Doty for technical assistance; and Colleen Nelson, Jason Wilson, and Jeff Zeznik for access to robotics equipment at the British Columbia Prostate Research Centre. This work was supported by grants from the National Cancer Institute of Canada (to M.R.), Uniformed Services University of the Health Sciences Grant R071GW (to T.D.), and National Institutes of Health Grant CA16519 (to P.H.). K.B. was supported by Postdoctoral Fellowships from the Canadian Institute of Health Research and the Michael Smith Foundation for Health Research.

1. Mayer, T. U., Kapoor, T. M., Haggarty, S. J., King, R. W., Schreiber, S. L. & Mitchison, T. J. (1999) *Science* **286,** 971–974.
2. Roskelley, C. D., Williams, D. E., McHardy, L. M., Leong, K. G., Troussard, A., Karsan, A., Andersen, R. J., Dedhar, S. & Roberge, M. (2001) *Cancer Res.* **61,** 6788–6794.
3. Lokey, R. S. (2003) *Curr. Opin. Chem. Biol.* **7,** 91–96.
4. Hughes, T. R. (2002) *Funct. Integr. Genomics* **2,** 199–211.
5. Parsons, A. B., Geyer, R., Hughes, T. R. & Boone, C. (2003) *Prog. Cell Cycle Res.* **5,** 159–166.
6. Giaever, G., Shoemaker, D. D., Jones, T. W., Liang, H., Winzeler, E. A., Astromoff, A. & Davis, R. W. (1999) *Nat. Genet.* **21,** 278–283.
7. Williams, D. E., Craig, K. S., Patrick, B., McHardy, L. M., van Soest, R., Roberge, M. & Andersen, R. J. (2002) *J. Org. Chem.* **67,** 245–258.
8. Winzeler, E. A., Shoemaker, D. D., Astromoff, A., Liang, H., Anderson, K., Andre, B., Bangham, R., Benito, R., Boeke, J. D., Bussey, H., *et al.* (1999) *Science* **285,** 901–906.
9. Beeler, T., Bacikova, D., Gable, K., Hopkins, L., Johnson, C., Slife, H. & Dunn, T. (1998) *J. Biol. Chem.* **273,** 30688–30694.
10. Burke, D., Dawson, D. & Stearns, T. (2000) *Methods in Yeast Genetics* (Cold Spring Harbor Lab. Press, Plainview, NY).
11. Tong, A. H., Evangelista, M., Parsons, A. B., Xu, H., Bader, G. D., Page, N., Robinson, M., Raghibizadeh, S., Hogue, C. W., Bussey, H., *et al.* (2001) *Science* **294,** 2364–2368.
12. Amberg, D. C. (1998) *Mol. Biol. Cell* **9,** 3259–3262.
13. Ohanian, J. & Ohanian, V. (2001) *Cell. Mol. Life Sci.* **58,** 2053–2068.
14. Dickson, R. C. & Lester, R. L. (2002) *Biochim. Biophys. Acta* **1583,** 13–25.
15. Casamayor, A., Torrance, P. D., Kobayashi, T., Thorner, J. & Alessi, D. R. (1999) *Curr. Biol.* **9,** 186–197.
16. Inagaki, M., Schmelzle, T., Yamaguchi, K., Irie, K., Hall, M. N. & Matsumoto, K. (1999) *Mol. Biol. Cell* **19,** 8344–8352.
17. Zanolari, B., Friant, S., Funato, K., Sutterlin, C., Stevenson, B. J. & Riezman, H. (2000) *EMBO J.* **19,** 2824–2833.
18. Beeler, T. J., Fu, D., Rivera, J., Monaghan, E., Gable, K. & Dunn, T. M. (1997) *Mol. Gen. Genet.* **255,** 570–579.
19. Zhao, C., Beeler, T. & Dunn, T. (1994) *J. Biol. Chem.* **269,** 21480–21488.
20. Ruvolo, P. P. (2003) *Pharmacol. Res.* **47,** 383–392.
21. Parsons, A. B., Brost, R. L., Ding, H., Li, Z., Zhang, C., Sheikh, B., Brown, G. W., Kane, P. M., Hughes, T. R. & Boone, C. (2004) *Nat. Biotechnol.* **22,** 62–69.
22. Lum, P. K., Armour, C. D., Stepaniants, S. B., Cavet, G., Wolf, M. K., Butler, J. S., Hinshaw, J. C., Garnier, P., Prestwich, G. D., Leonardson, A., *et al.* (2004) *Cell* **116,** 121–137.
23. Collins, F. S., Green, E. D., Guttmacher, A. E. & Guyer, M. S. (2003) *Nature* **422,** 835–847.